Scientific Research Publishing

Journal of Applied Mathematics and Physics, 2025, 13(2), 525-552
https://www.scirp.org/journal/jamp
ISSN Online: 2327-4379
ISSN Print: 2327-4352

Dynamics of a Class of Multiple Sclerosis Models with Saturated Activation Rates of T Cells

Yu Su

School of Mathematics and Statistics, Northwest Normal University, Lanzhou, China
Email: 1982933472qq.com

How to cite this paper: Su, Y. (2025) Dynamics of a Class of Multiple Sclerosis Models with Saturated Activation Rates of T Cells. *Journal of Applied Mathematics and Physics*, **13**, 525-552.
https://doi.org/10.4236/jamp.2025.132029

Received: January 20, 2025
Accepted: February 22, 2025
Published: February 25, 2025

Abstract

Many autoimmune diseases exhibit an alternating pattern of relapses and remissions in which the apparent self-tolerance phase is interrupted by periodic autoimmune episodes. In this paper, we introduce a class of terminally differentiated effector T cells to an existing model of autoimmune disease and investigate the stability and Hopf branching phenomenon in a model of multiple sclerosis with a saturable functional response. First, we explore the local asymptotic stability of the equilibrium point and propose conditions for the existence of Hopf branching. Finally, with the help of canonical type theory and the central manifold theorem, we analyze the direction of Hopf branching and the stability of branching periodic solutions.

Keywords

Multiple Sclerosis Model, Saturated Functional Response, Equilibrium Point, Stability, Hopf Bifurcation

1. Introduction

T cells occupy a pivotal position in the establishment and preservation of the immune system [1], and they are acknowledged as pivotal factors in numerous inflammatory and autoimmune disorders. The *in vivo* functions of T cells within the realms of immunology and immunopathology, along with their underlying mechanisms, have undergone extensive scrutiny [2]. These investigations have significantly propelled the advancement of immune-based therapies, particularly those aimed at effector T cells (Teff) and regulatory T cells (Treg). Effector T cells are tasked with identifying and eliminating pathogens or virus-infected cells. Meanwhile, regulatory T cells are categorized into natural (nTreg) and induced

(iTreg) subtypes, playing a crucial role in the prevention of autoimmune diseases and the modulation of effector T cell function. The receptors on the surface of T cells possess the capability to recognize a diverse array of antigens derived from pathogens, tumors, and the environment. Additionally, they maintain immune memory and self-tolerance. Naive T cells, equipped with specific antigen receptors, continuously circulate in the bloodstream and necessitate two conditions for activation: recognition of the corresponding antigen presented by antigen-presenting cells and engagement with co-stimulatory molecules on these cells. This intricate process is primarily orchestrated by specialized antigen-presenting cells, notably dendritic cells (DCs). In response to signals emanating from the innate immune system, immature dendritic cells capture antigenic peptides at the sites of infection or inflammation within tissues. This critical interaction triggers the initiation of an adaptive immune response, subsequently prompting the maturation of the dendritic cells. As they mature, these cells migrate towards peripheral lymphoid tissues, undergoing concurrent alterations in the expression patterns of their surface molecules, notably including co-stimulatory molecules. Concurrently, naive T cells are in continuous circulation within the peripheral lymphoid tissue, rapidly scanning and interacting with numerous dendritic cells. Upon recognition of a homologous antigen, these T cells establish stable interactions with the antigen-presenting dendritic cells. Consequently, the activated T cells cease their circulatory pattern, proliferating extensively within the peripheral lymphoid tissue. They primarily differentiate into effector T cells, a phase of immense importance as the initial subpopulation of T cells specific to a particular antigen is typically very small and must undergo significant expansion to mount an effective immune response. This proliferative process is driven by cytokines, such as interleukin-2 (IL-2), which are both produced and utilized by the activated T cells, along with sourcing it from other available pathways. After fully differentiating into effector cells, T cells are reintroduced into the bloodstream and migrate towards the site of infection to execute a "cell-mediated" adaptive immune response. The adaptive immune system comprises a series of highly specialized cells and processes, which are capable of restricting or eradicating foreign pathogens [3]. Normally, the immune system must respond to invading pathogens while refraining from attacking its own tissues; when this differentiation fails, autoimmune diseases arise.

Autoimmune diseases, such as multiple sclerosis (MS), are frequently modeled through the dynamics of T-cell interactions, yet their spatial characteristics and dynamics, which contribute to spatial heterogeneity, are often neglected. The immune system serves as the body's primary defense against pathogens [4], and the regulatory capacity of its cells is crucial in preventing inflammatory diseases, including MS. Multiple sclerosis is a disease impacting the central nervous system (comprising the brain, retina, and spinal cord), characterized by the formation of sclerotic plaques in these areas, resulting in partial or complete paralysis, muscle spasms, and various other symptoms [5]. In MS, the immune system attacks the

myelin sheath surrounding nerve axons, causing demyelination, which exposes the axons and disrupts signaling. This, in turn, leads to sensory and visual impairments, loss of motor skills, and cognitive deficiencies. Multiple sclerosis involves the interplay of T cells, B cells, and myeloid cells, such as macrophages, dendritic cells, oligodendrocytes, and monocytes [6]. The disease is categorized into relapsing-remitting MS (RRMS), primary progressive MS (PPMS), and secondary progressive MS (SPMS), with RRMS being the most prevalent form. It is characterized by sudden onset of neurological deficits followed by remission. MS can also be subclassified based on immunopathological features, including myelin protein loss, plaque distribution and extension, oligodendrocyte destruction, and immunoglobulin and complement activity [7].

In the realm of mathematical modeling focused on T-cell interactions in multiple sclerosis (MS), the ordinary differential equation (ODE) model for MS was initially introduced by Broome *et al.* in 2011, grounded in biochemical theory. Subsequently, in the same year, Alexander and Wahl [8] proposed their own ODE model (1.1) for MS, adopting an innovative methodology to isolate the effects of immunosuppression mediated by a specific Treg mechanism within a given system. These authors emphasize the pivotal role of professional antigen-presenting cells (PAPCs), explicitly incorporating them as dynamic system variables, thereby highlighting their intrinsic significance. This novel approach also facilitates the modeling of a sophisticated positive feedback mechanism: effector T cells trigger the release of antigens, which are subsequently engulfed by immature PAPCs. These PAPCs then mature into fully functional antigen-presenting cells, further stimulating the generation of effector T cells. To explore three plausible Treg action mechanisms, an ODE model was formulated. Both antigen-specific Tregs and arbitrary-specific Tregs suppress the immune response directed against a particular autoantigen by acting on mature PAPCs or autoreactive effector T cells. Within this framework, the authors derive the equilibrium state and assess its stability by computing the basic regeneration ratio R. They elucidate that the absence of a self-injurious cell population in a normal equilibrium signifies a state of self-tolerance, whereas its presence in a non-trivial equilibrium indicates a condition of chronic autoimmunity. System 1 (1.1) assumes that antigen uptake occurs linearly, and System 2 assumes that antigen uptake is controlled by Mie kinetics, *i.e.* $\tilde{\nu}G$ in System 1 becomes $\frac{\tilde{\nu}G}{k+G}$.

$$\begin{cases} \dot{A} = f\tilde{\nu}G - \left(\sigma_1 R + b_1\right)A - \mu_A A, \\ \dot{R} = \left(\pi_1 E + \beta\right)A - \mu_R R, \\ \dot{E} = \lambda_E A - \mu_E E, \\ \dot{G} = \gamma E - \tilde{\nu}G - \mu_G G, \end{cases} \tag{1.1}$$

where A is the mature specialized antigen-presenting cell (PAPC), a class of immune cells whose role is to activate T cells to present antigens to lymphocytes; R is the reactive regulatory T cell (Treg); E is the reactive effector (regular)

T cell (Teff), and these are likely to be $CD4^+$; G is the reactive effector of a specific self-antigen, G; G is the reactive effector of a specific self-antigen, G. Specific self-antigens, *i.e.* antigens released by host cells; f the proportion of mature PAPC uptake of antigens $(0 \le f \le 1)$; $\tilde{v}$ is the rate at which immature PAPC uptake of antigens takes place; σ_1 is the rate at which A is inhibited by Treg; b_1 is the rate at which A b_1 is the rate of A inhibition by other cells; μ_A is the rate of A apoptosis; π_1 is the rate of R activation by A in E due to IL-2 autocrine in Teff; β is the rate of R activation by A due to IL-2 autocrine in PAPC; μ_R is the rate of R apoptosis; λ_E is the rate of A activation of E; μ_E is the rate of E apoptosis; γ is the rate of release of G in E; μ_G is the rate of G apoptosis.

In 2014, Zhang, Wahl, and Yu [9] [10] enhanced System 1 by acknowledging that the model proposed by H.K. Alexander and L.M. Wahl accurately portrays the inherent feedback mechanism of autoimmunity. In this mechanism, plasmacytoid antigen-presenting cells (PAPCs) exhibit self-antigens, which stimulate self-reactive effector T cells. These T cells subsequently attack host cells, causing damage that results in an elevated concentration of self-antigens. This, in turn, activates more PAPCs. Experimental evidence has demonstrated the significant importance of HLA-DR+ cells. Consequently, W.J. Zhang, L.M. Wahl, and P. Yu expanded the existing model (1.1) to incorporate this class of potently inhibitory cells, modeling HLA-DR+ as a novel type of regulatory T cell (Treg).

The remainder of the paper proceeds as follows: In the second part, the model (1.1) undergoes transformation. Considering the activation rate of nTreg as $(\pi_1 E + \beta)A$, this section assumes a saturated state of nTreg activation, transforming EA into the saturated form $\frac{aEA}{1+bE}$ [11] termed as the saturation incidence. Subsequently, the equilibrium point of the new model is computed. Part III delves into the stability analysis of the new model away from its equilibrium point, deriving the conditions for stability and identifying the critical point for the onset of Hopf bifurcation. The fourth part discusses the direction of the Hopf branch and the stability of the periodic solution, utilizing the central manifold theorem and the canonical type method. Numerical simulations are employed in the fifth part to validate the results presented in this paper. Finally, a brief discussion on the findings of this paper is provided. In this section, the saturation activation rate of effector T cells $f(A,E) = \frac{aEA}{1+bE}$ is introduced [12], transforming model (1.1) into the following model.

$$\begin{cases} \dot{A} = f\tilde{v}G - (\sigma_1 R + b_1)A - \mu_A A, \\ \dot{R} = \frac{\pi_1 aEA}{1+bE} + \beta A - \mu_R R, \\ \dot{E} = \lambda_E A - \mu_E E, \\ \dot{G} = \gamma E - \tilde{v}G - \mu_G G, \end{cases} \tag{1.2}$$

Approximate (1.2) such that $x = \varepsilon A$, $y = \xi R$, $w = \eta E$, $z = \alpha G$, $\tau = \delta t$,

Substituting t for τ, we obtain the following model.

$$\begin{cases} \dfrac{\mathrm{d}x}{\mathrm{d}t} = nz - mxy - x, \\ \dfrac{\mathrm{d}y}{\mathrm{d}t} = \dfrac{cxw}{1+w} + x - dy, \\ \dfrac{\mathrm{d}w}{\mathrm{d}t} = x - ew, \\ \dfrac{\mathrm{d}z}{\mathrm{d}t} = w - hz, \end{cases} \tag{1.3}$$

where $\varepsilon = \dfrac{b\lambda_E}{b_1 + \mu_A}$, $\xi = \dfrac{b\lambda_E}{\beta}$, $\eta = b$, $\alpha = \dfrac{b\left(b_1 + \mu_A\right)}{\gamma}$, $\delta = b_1 + \mu_A$, $n = \dfrac{b\lambda_E \gamma f\tilde{v}}{\left(b_1 + \mu_A\right)^3}$, $m = \dfrac{\sigma_1 \beta}{\left(b_1 + \mu_A\right) b\lambda_E}$, $c = \dfrac{a\pi_1}{\beta b}$, $d = \dfrac{\mu_R}{b_1 + \mu_A}$, $e = \dfrac{\mu_E}{b_1 + \mu_A}$, $h = \dfrac{\tilde{v} + \mu_G}{b_1 + \mu_A}$.

x indicates specialized antigen-presenting cells, y indicates activity-regulating T cells; w indicates active effector T cells; z indicates specific self-antigens, *i.e.* antigens released by host cells. n: parameter related to antigen uptake and PAPC activation, reflecting the efficiency with which antigen is taken up by PAPC and activated, *m*: reflecting the strength of inhibition of PAPC by Treg, *c*: parameter related to antigen release and PAPC activation in Teff, which may involve the processes of antigen processing, presentation and recognition, *d*: reflecting the rate of decline of Treg or the interaction with other cells resulting in a reduction. *e*: Parameters related to antigen release and Teff growth that may involve processes of Teff proliferation and activation, *h*: reflects the rate of decline of the antigen or the mechanism of its clearance. Influence of parameters on systemic behavior: an increase in *n* promotes the activation of PAPC and the growth of Teff, thus enhancing the immune response, an increase in *m* strengthens the inhibitory effect of Treg on PAPC and may lead to a weakening of the immune response, a change in c may affect the activation of Teff and the release of antigens, which in turn affects the strength and duration of the immune response, and an increase in *d* leads to a decrease in Treg number which may weaken immune regulation and make the immune response more intense, *e*: an increase in *e* promotes Teff growth and antigen clearance, contributing to a rapid and effective immune response, *h*: an increase in *h* accelerates the clearance of antigens but may lead to a premature termination of the immune response. Interaction between cells: PAPC (x) initiates the immune response by taking up antigens and activating Teff (w), Treg (y) regulates the immune response by inhibiting PAPC to prevent autoimmune disease caused by over-activation, Teff (w) proliferates and clears the infected or abnormal cells under the stimulation of antigen and is the main executor of the immune response, antigen (z) acts as a triggering factor, and changes in the concentration of antigen directly affect the immune response. Concentration changes directly affect the intensity and duration of the immune response. Together, these parameters and cell-cell interactions determine the dynamic

behavior of the immune system, including the initiation, regulation, and termination processes of the immune response. By adjusting these parameters, it is possible to study the response characteristics of the immune system under different conditions and provide a theoretical basis for disease treatment and immune regulation.

The biological rationale for the inclusion of a saturated functional response is mainly reflected in the following aspects:

1) More accurate modeling of the dynamic interactions of immune cells with antigens:

The original model, while capable of describing the basic interactions of immune cells with antigens in multiple sclerosis (MS), fails to adequately take into account the nonlinear relationship between the rate of immune cell response and changes in antigen concentration.

The saturated functional response function introduces this nonlinear relationship, *i.e.* the response rate of immune cells increases and then decreases with increasing antigen concentration, which is more in line with the biological reality.

2) Reflecting the inhibitory state of immune cells:

At high antigen concentrations, the response rate of immune cells decreases, which reflects the inhibitory state of immune cells that may occur after prolonged exposure to antigens and is an important factor in the exacerbation of MS.

The original model failed to reflect this, and with the addition of a saturated functional response, the model was able to more accurately describe this phenomenon.

3) Consideration of competition and inhibition between immune cells:

The saturation-type functional response not only takes into account the effect of antigen concentration on the response rate of immune cells, but also implicitly considers competition and inhibition between immune cells.

This is particularly important in MS, where complex regulatory mechanisms between immune cells have a critical impact on disease progression.

The biological significance of the inclusion of a saturated functional response is:

1) Improves the accuracy and utility of the model, allowing it to shed more light on the pathomechanisms of MS.

2) Provides a powerful tool for understanding the disease progression and therapeutic strategies in MS by modeling the dynamic interactions between immune cells and antigens.

It helps researchers to better understand the behavior of immune cells in the process of MS and provides a theoretical basis for the development of new therapeutic approaches.

2. Existence and Stability of Equilibrium Points

2.1. Existence of Equilibrium Points

Theorem 1: For system (1.3), there is a trivial equilibrium solution $E_0 = (0,0,0,0)$; when $n > eh$ system (1.3) has a unique nontrivial equilibrium solution

$E^* = (x^*, y^*, w^*, z^*)$. We write system (1.3) in the following form.

$$\begin{cases} \dfrac{\mathrm{d}x}{\mathrm{d}t} = nz - mxy - x \triangleq f_1(x,y,w,z), \\ \dfrac{\mathrm{d}y}{\mathrm{d}t} = \dfrac{cxw}{1+w} + x - dy \triangleq f_2(x,y,w,z), \\ \dfrac{\mathrm{d}w}{\mathrm{d}t} = x - ew \triangleq f_3(x,y,w,z), \\ \dfrac{\mathrm{d}z}{\mathrm{d}t} = w - hz \triangleq f_4(x,y,w,z), \end{cases} \tag{2.1}$$

Let the right end of the above system be equal to 0, to obtain

$$z(n - mehy - eh) = 0, cehz\frac{hz}{1+hz} + ehz - dy = 0. \tag{2.2}$$

which gives $z = 0$ or $n - mehy - eh = 0$. Thus, a trivial equilibrium solution $E_0 = (0,0,0,0)$ can be obtained. On the other hand, the solution $y = \dfrac{n-eh}{meh}$, which carries $cehz\dfrac{hz}{1+hz} + ehz - dy = 0$ leads to

$$me^2h^3(c+1)z^2 + (edh^2 + me^2h^2 - ndh)z + edh - nd = 0. \tag{2.3}$$

When $\Delta = (edh^2 + me^2h^2 - ndh)^2 - 4me^2h^3(c+1)(edh - nd) > 0$, that is, when $n > eh \triangleq n_2$, the above equation has two solutions

$$z_1^* = \frac{-(edh + me^2h - nd) + \sqrt{(edh + me^2h - nd)^2 - 4me^2h(c+1)(edh - nd)}}{2me^2h^2(c+1)},$$

$$z_2^* = \frac{-(edh + me^2h - nd) - \sqrt{(edh + me^2h - nd)^2 - 4me^2h(c+1)(edh - nd)}}{2me^2h^2(c+1)}.$$

It is also known from the original system $x_i^* = ehz_i^*$, $w_i^* = hz_i^*$, $y^* \triangleq y = \dfrac{n-eh}{meh}$, $i = 1,2$, that when $edh + me^2h - nd \geq 0$, *i.e.* $n \leq eh + \dfrac{me^2h}{d} \triangleq n_1$ when, $z_1^* > 0$, $z_2^* < 0$; when $edh + me^2h - nd < 0$, $n > \triangleq n_1$, $z_1^* > 0$, $z_2^* < 0$. In summary, z_1^* is positive when $n_2 < n < n_1$ or $n > n_1$. Notation $z^* \triangleq z_1^*$, $x^* \triangleq x_1^* = ehz_1^*$, $w^* \triangleq w_1^* = hz_1^*$, $y^* \triangleq y = \dfrac{n-eh}{meh}$. Thus, a nontrivial equilibrium solution of the system can be obtained $E^* = (x^*, y^*, w^*, z^*)$.

2.2. Local Stability of the Equilibrium Solution of the System

The jacobi matrix and the characteristic equation of the system (1.3):

$$J = \begin{pmatrix} -1 - my & -mx & 0 & n \\ 1 + \dfrac{cw}{1+w} & -d & \dfrac{cx}{(1+w)^2} & 0 \\ 1 & 0 & -e & 0 \\ 0 & 0 & 1 & -h \end{pmatrix}.$$

$$J(\lambda)=\begin{vmatrix} \lambda+1+my & mx & 0 & -n \\ -1-\dfrac{cw}{1+w} & \lambda+d & -\dfrac{cx}{(1+w)^2} & 0 \\ -1 & 0 & \lambda+e & 0 \\ 0 & 0 & -1 & \lambda+h \end{vmatrix}.$$

$$J(\lambda)=-n(\lambda+d)+(\lambda+h)\left[(\lambda+e)(\lambda+d)(\lambda+1+my)+\frac{cmx^2}{(1+w)^2}+mx(\lambda+e)\left(1+\frac{cw}{1+w}\right)\right]=0$$

Theorem 2: System (1.1) is locally asymptotically stable at E_0 if the condition $n<n_2$ is satisfied, and unstable if $n>n_2$.

Proof: the Jacobi matrix for system (1.3) at E_0 is

$$J_{E_0}=\begin{pmatrix} -1 & 0 & 0 & n \\ 1 & -d & 0 & 0 \\ 1 & 0 & -e & 0 \\ 0 & 0 & 1 & -h \end{pmatrix}.$$

The characteristic equation is $(\lambda+d)\left[\lambda^3+A_1\lambda^2+A_2\lambda+A_3\right]=0$, where $A_1=1+e+h$, $A_2=eh+h+e$, $A_3=eh-n$. can be obtained as $\lambda_1=-d$. For $\lambda^3+A_1\lambda^2+A_2\lambda+A_3=0$, using the Hurwitz criterion:

1) When $n<n_2$, $A_1,A_2,A_3>0$, and $\Delta_2=A_1A_2-A_3>0$, thus all characteristic roots of the characteristic equation have negative real parts, so that the system (1.3) is locally and asymptotically stabilized at the zero equilibrium solution;

2) When $n>n_2$, $A_3<0$, so the system (1.3) is unstable at the zero equilibrium solution.

The stability of system (1.3) at E^* is discussed below. The characteristic equation for system (1.3) at E^* is

$$\lambda^4+B_1\lambda^3+B_2\lambda^2+B_3\lambda+B_4=0. \tag{2.4}$$

where

$$B_1=h+d+e+my^*+1,$$

$$B_2=eh+dh+h+mhy^*+ed+e+emy^*+d+mdy^*+mx^*+\frac{cmx^*}{1+w^*},$$

$$B_3=edh+emhy^*+eh+mdhy^*+ed+dh+medy^*+\frac{cmx^{*2}}{(1+w^*)^2}$$
$$+mex^*+mhx^*+\frac{cmhx^*w^*}{1+w^*}+\frac{cmex^*w^*}{1+w^*}-n$$

$$B_4=edh+edhmy^*+emhx^*+\frac{cmhx^{*2}}{(1+w^*)^2}+\frac{cmehx^*w^*}{1+w^*}-nd$$

Using the *Hurwitz* criterion, since $y^*=\dfrac{n-eh}{meh}$, it follows that $B_3,B_4>0$, and since $B_1,B_2>0$, the system (1.3) is locally asymptotically stable at E^*, The system (1.3) is locally asymptotically stable at E^* when

$\Delta_3 = \left(B_1 B_2 - B_3\right) B_3 - B_1^2 B_4 > 0$.

3. Existence of a Hopf Bifurcation of the System

Lemma 1: Suppose that given a system

$$\dot{x} = f_\mu(x), x \in \mathbb{R}^n, \mu \in \mathbb{R}$$

There exists an equilibrium point (x_0, μ_0), and the system undergoes *Hopf* branching at the equilibrium point (x_0, μ_0), when the system satisfies the following conditions.

1) $D_x f_{u_0}(x_0)$ has a pair of conjugate pure imaginary roots $\lambda(\mu)$ and $\bar{\lambda}(\mu)$, and the real parts of $n-2$ eigenvalues other than the pair of conjugate pure imaginary root eigenvalues are all less than zero.

2) $\dfrac{\mathrm{d}}{\mathrm{d}\mu}\left(Re\left(\lambda(u)\right)\right)\Big|_{\mu=\mu_0} \neq 0$.

Theorem 3: *Hopf* branching existence theorem. Let

$$B_1 = h + d + e + my^* + 1,$$

$$B_2 = eh + dh + h + mhy^* + ed + e + emy^* + d + mdy^* + mx^* + \frac{cmx^*}{1+w^*},$$

$$B_3 = edh + emhy^* + eh + mdhy^* + ed + dh + medy^* + \frac{cmx^{*2}}{\left(1+w^*\right)^2} + mex^* + mhx^* + \frac{cmhx^*w^*}{1+w^*} + \frac{cmex^*w^*}{1+w^*} - n$$

$$B_4 = edh + edhmy^* + emhx^* + \frac{cmhx^{*2}}{\left(1+w^*\right)^2} + \frac{cmehx^*w^*}{1+w^*} - nd$$

Under the condition that the positive equilibrium point $E^* = \left(x^*, y^*, w^*, z^*\right)$ exists, if the parameters satisfy when the

1) $a_1^2 d + 2x_1 - a_1 a_2 > 0$, *i.e.* $a_2 < \dfrac{a_1^2 d + 2x_1}{a_1}$ (H_1), when H_1 is satisfied, $n_1 > 0$ is constant.

2) Under the condition of H_1, if $a_1^2 x_2 + x_1^2 - a_1 a_2 x_1 > 0$, *i.e.* $a_2 < \dfrac{a_1^2 x_2 + x_1^2}{a_2 x_1}$ (H_2), then take $\min\{H_1, H_2\}$, when $a_2 < \min\{H_1, H_2\}$, $n_2 > 0$ is always true.

3) $a_1^2 d + 2x_1 - a_1 a_2 < 0$, *i.e.* $a_2 > \dfrac{a_1^2 d + 2x_1}{a_1}$ (H_3), if $a_1^2 x_2 + x_1^2 - a_1 a_2 x_1 < 0$, *i.e.* $a_2 > \dfrac{a_1^2 x_2 + x_1^2}{a_1 x_1}$ (H_4), take $\max\{H_3, H_4\}$, when $a_2 > \max\{H_3', H_4'\}$, $n_1 > 0$ is constant. Then, when the parameter n changes and crosses the critical value

$$n_1 = \frac{\left(a_1^2 d + 2x_1 - a_1 a_2\right) + \sqrt{\left(a_1 a_2 - a_1^2 d - 2x_1\right)^2 - 4\left(a_1^2 x_2 + x_1^2 - a_1 a_2 x_1\right)}}{2},$$

$$n_2 = \frac{\left(a_1^2 d + 2x_1 - a_1 a_2\right) - \sqrt{\left(a_1 a_2 - a_1^2 d - 2x_1\right)^2 - 4\left(a_1^2 x_2 + x_1^2 - a_1 a_2 x_1\right)}}{2}.$$

the system (1.3) branches *Hopf* at the equilibrium point $E^* = \left(x^*, y^*, w^*, z^*\right)$.

Proof: Let the characteristic equation (2.4) of the system (1.3) at the equilibrium point E^* have a pair of purely imaginary characteristic roots $\lambda = \pm \mathrm{i}\omega$, and bringing the purely imaginary roots $\mathrm{i}\omega$ into the characteristic equation yields

$$(\mathrm{i}\omega)^4 + B_1(\mathrm{i}\omega)^3 + B_2(\mathrm{i}\omega)^2 + B_3\mathrm{i}\omega + B_4 = 0$$

Separating the real and imaginary parts yields

$$\begin{cases} \omega^4 - B_2\omega^2 + B_4 = 0 \\ B_1\omega^3 - B_3\omega = 0 \end{cases} \tag{3.1}$$

According to the second equation of (3.1), we get $\omega = \omega_0 = \sqrt{\frac{B_3}{B_1}}$

Choose n as the branching parameter, so that $B_3 = x_1 - n$, $B_4 = x_2 - nd$.

$$x_1 = edh + emhy^* + eh + mdhy^* + ed + dh + medy^* + \frac{cmx^{*2}}{\left(1+w^*\right)^2}$$

$$+ mex^* + mhx^* + \frac{cmhx^*w^*}{1+w^*} + \frac{cmex^*w^*}{1+w^*}$$

$$x_2 = edh + edhmy^* + emhx^* + \frac{cmhx^{*2}}{\left(1+w^*\right)^2} + \frac{cmehx^*w^*}{1+w^*}$$

Substituting $\omega = \omega_0 = \sqrt{\frac{B_3}{B_1}}$ into the first Equation of (3.1), we have

$$\left(\frac{B_3}{B_1}\right)^2 - B_2\frac{B_3}{B_1} + B_4 = 0$$

Substituting and organizing B_3, B_4 yields

$$\left(x_1 - n\right)^2 - B_1B_2\left(x_1 - n\right) + \left(B_1\right)^2 B_4 = 0$$

The quadratic equation organized as a quadratic equation about n has

$$n^2 - \left(a_1^2 d + 2x_1 - a_1 a_2\right) + a_1^2 x_2 + x_1^2 - a_1 a_2 x_1 = 0$$

Solving the above equation leads to the theorem n_1, n_2, The three conditions in the theorem are preconditions to ensure that the branching parameter is greater than zero.

At this point, the branching parameter $n = n_{1(2)}$ is substituted into the characteristic equation, and according to Vedda's theorem, the four roots of the characteristic equation can be found to be [13]

$$\lambda_1 = \mathrm{i}\omega_0, \lambda_2 = -\mathrm{i}\omega_0 \left(\omega_0 = \sqrt{\frac{B_3}{B_1}}\right)$$

$$\lambda_3 = \frac{-B_1 + \sqrt{B_1^2 - 4\left(B_2 - \frac{B_3}{B_1}\right)}}{2}, \lambda_4 = \frac{-B_1 - \sqrt{B_1^2 - 4\left(B_2 - \frac{B_3}{B_1}\right)}}{2}.$$

Thus, system (1.3) satisfies the first condition in Lemma 1 for the existence of *Hopf* branches when the parameters satisfy the conditions for the existence of positive equilibria and the conditions in Theorem 3.

According to the characteristic Equation (2.4), the partial derivatives of the characteristic equation with respect to the parameter n are given by

$$\left[4\lambda^3+3B_1\lambda^2+2B_2\lambda\right]\frac{\partial_\lambda}{\partial_n}-\lambda+B_3\frac{\partial_\lambda}{\partial_n}-d=0$$

Organizing the above equation gives

$$\left[4\lambda^3+3B_1\lambda^2+2B_2\lambda+B_3\right]\frac{\partial_\lambda}{\partial_n}=\lambda+d$$

$$\frac{\partial_\lambda}{\partial_n}=\frac{\lambda+d}{4\lambda^3+3B_1\lambda^2+2B_2\lambda+B_3}\Bigg|_{\lambda=\mathrm{i}\omega_0}$$

happening

$$\frac{\partial_\lambda}{\partial_n}\left(n_0\right)=\frac{d+\mathrm{i}\omega_0}{\left(B_3-3B_1\omega_0^2\right)+\left(2B_2\omega_0-4\omega_0^3\right)\mathrm{i}}$$

Since $d>0$, *i.e.*

$$Re\left(\frac{\partial_\lambda}{\partial_n}\left(n_0\right)\right)=\frac{\left(B_3-3B_1\omega_0^2\right)d+\left(2B_2\omega_0^2-4\omega_0^4\right)}{\left(B_3-3B_1\omega_0^2\right)^2+\left(2B_2\omega_0-4\omega_0^3\right)^2}\neq 0$$

Therefore, a *Hopf* bifurcation occurs at the equilibrium point $E^*=\left(x^*,y^*,w^*,z^*\right)$.

4. Stability and Direction of the System Hopf Bifurcation

This section discusses the direction and stability [14] [15] of the Hopf bifurcation of the system (1.3) arising near the normal number equilibrium point E^* using canonical type theory and projection methods. Variable substitution for the system (1.3)

$$\tilde{x}=x-x^*,\tilde{y}=y-y^*,\tilde{w}=w-w^*,\tilde{z}=z-z^*$$

The transformation is still replaced by u,v,w,x. $\tilde{u},\tilde{v},\tilde{w},\tilde{x}$. Then, the system (1.3) becomes

$$\begin{cases}\dfrac{\mathrm{d}x}{\mathrm{d}t}=n\left(z+z^*\right)-m\left(x+x^*\right)\left(y+y^*\right)-\left(x+x^*\right),\\ \dfrac{\mathrm{d}y}{\mathrm{d}t}=\dfrac{c\left(x+x^*\right)\left(w+w^*\right)}{1+\left(w+w^*\right)}+\left(x+x^*\right)-d\left(y+y^*\right),\\ \dfrac{\mathrm{d}w}{\mathrm{d}t}=\left(x+x^*\right)-e\left(w+w^*\right),\\ \dfrac{\mathrm{d}z}{\mathrm{d}t}=\left(w+w^*\right)-h\left(z+z^*\right),\end{cases}\tag{4.1}$$

Therefore, the positive equilibrium point $E^*=\left(x^*,y^*,w^*,z^*\right)$ of the model (1.3) becomes the zero point (0, 0, 0, 0) of the system (4.1), and the system (4.1)

becomes

$$\frac{\mathrm{d}\boldsymbol{U}}{\mathrm{d}t}=\boldsymbol{J}_{E^*}\boldsymbol{U}+\boldsymbol{F}(\boldsymbol{U})+\frac{1}{2}\boldsymbol{B}(\boldsymbol{x},\boldsymbol{y})+\frac{1}{6}\boldsymbol{C}(\boldsymbol{x},\boldsymbol{y},\boldsymbol{z})+\cdots, \tag{4.2}$$

where

$$\boldsymbol{U}=(x,y,w,z)^{\mathrm{T}},\quad \boldsymbol{F}(\boldsymbol{U})=(F_1,F_2,F_3,F_4)^{\mathrm{T}}.$$

The components of $\boldsymbol{F}(\boldsymbol{U})$ are as follows:

$$F_1=-mxy+\cdots,$$

$$F_2=\frac{c}{\left(1+w^*\right)^2}xw-\frac{cx^*}{\left(1+w^*\right)^3}w^2-\frac{c}{\left(1+w^*\right)^3}xw^2+\frac{cx^*}{\left(1+w^*\right)^4}w^3+\cdots,$$

$$F_3=0,$$

$$F_4=0.$$

When $n=n^*_{1(2)}$, the eigenvalues of the system (1.3) at the equilibrium point E^* are $\lambda_{1,2}=\dfrac{-B_1\pm\sqrt{B_1^2-4\left(B_2-\dfrac{B_3}{B_1}\right)}}{2}$, $\lambda_{3,4}=\pm i\omega_0\left(\omega_0=\sqrt{\dfrac{B_3}{B_1}}\right)$. Let $\lambda_{1,2}\neq 0$, $\boldsymbol{J}_{\boldsymbol{E}}^*$ and $\boldsymbol{J}_{\boldsymbol{E}}^{*\mathrm{T}}$ have eigenvectors corresponding to pure imaginary roots when the eigenvalues of $\boldsymbol{q}$ and $\boldsymbol{p}$ satisfy

$$\boldsymbol{J}_{\boldsymbol{E}}^*\boldsymbol{q}=i\omega_0\boldsymbol{q},\quad \boldsymbol{J}_{\boldsymbol{E}}^{*\mathrm{T}}\boldsymbol{p}=-i\omega_0\boldsymbol{p}.$$

Let the fourth element of the matrix p,q be 1, we get

$$\boldsymbol{p}=\begin{pmatrix}\dfrac{h-i\omega_0}{n}\\ -\dfrac{mx^*\left(h-i\omega_0\right)}{n\left(d-i\omega_0\right)}\\ \dfrac{\left(h-i\omega_0\right)\left[\left(1+my^*-i\omega_0\right)+mx^*\left(cw^*+w^*+1\right)\right]}{n\left(1+w^*\right)\left(d-i\omega_0\right)}\\ 1\end{pmatrix}$$

$$\boldsymbol{q}=\begin{pmatrix}\left(e+i\omega_0\right)\left(h+i\omega_0\right)\\ \dfrac{-\left(1+my^*+i\omega_0\right)\left(e+i\omega_0\right)\left(h+i\omega_0\right)+n}{mx^*}\\ h+i\omega_0\\ 1\end{pmatrix},$$

command $\boldsymbol{q}^*=\boldsymbol{q}$, $\mu=\langle\boldsymbol{p},\boldsymbol{q}\rangle$, take $\boldsymbol{p}^*=\boldsymbol{p}\dfrac{1}{\mu}$. At this point, it satisfies

$$\mu=\mu_1+\mu_2+\mu_3+\mu_4,$$

$$\left\langle\boldsymbol{p}^*,\boldsymbol{q}^*\right\rangle=1,$$

$$\left\langle\overline{\boldsymbol{p}}^*,\boldsymbol{q}^*\right\rangle=\left\langle\boldsymbol{p}^*,\overline{\boldsymbol{q}}^*\right\rangle=0.$$

where

$$\mu_1 = \frac{(h-i\omega_0)^2(e-i\omega_0)(d-i\omega_0)(1+w^*)}{n(1+w^*)(d-i\omega_0)}$$

$$\mu_2 = \frac{\left[(1+my^*-i\omega_0)(e-i\omega_0)(h-i\omega_0)-n\right](h-i\omega_0)(1+w^*)}{n(1+w^*)(d-i\omega_0)}$$

$$\mu_3 = \frac{(h-i\omega_0)^2\left[(1+my^*-i\omega_0)+mx^*(cw^*+w^*+1)\right]}{n(1+w^*)(d-i\omega_0)},$$

$$\mu_4 = 1.$$

$$\overline{\boldsymbol{q}}^* = \begin{pmatrix} (e-i\omega_0)(h-i\omega_0) \\ \dfrac{-(1+my^*-i\omega_0)(e-i\omega_0)(h-i\omega_0)+n}{mx^*} \\ h-i\omega_0 \\ 1 \end{pmatrix},$$

$\overline{\boldsymbol{p}}^*$ and $\overline{\boldsymbol{q}}^*$ are respectively $\boldsymbol{p}^*$ and $\boldsymbol{q}^*$ of the covariance matrix, $\langle\,\rangle$ is the sign of the inner product. According to the nonlinear terms of the system (4.2), take the symmetric multilinear vector function with respect to $\boldsymbol{x}=(x_1,x_2,x_3,x_4)^{\mathrm{T}}$, $\boldsymbol{y}=(y_1,y_2,y_3,y_4)^{\mathrm{T}}$, $\boldsymbol{z}=(z_1,z_2,z_3,z_4)^{\mathrm{T}}$ of symmetric multilinear vector functions

$$\boldsymbol{B}(\boldsymbol{x},\boldsymbol{y}) = \begin{pmatrix} -m(x_1y_2+x_2y_1) \\ \dfrac{c}{(1+w^*)^2}(x_1y_3+x_3y_1)-\dfrac{2cx^*}{(1+w^*)^3}x_3y_3 \\ 0 \\ 0 \end{pmatrix}, \tag{4.3}$$

$$\boldsymbol{C}(\boldsymbol{x},\boldsymbol{y},\boldsymbol{z}) = \begin{pmatrix} 0 \\ -\dfrac{2c}{(1+w^*)^3}(x_1y_3z_3+x_3y_1z_3+x_3y_3z_1)+\dfrac{6cx^*}{(1+w^*)^4}x_3y_3z_3 \\ 0 \\ 0 \end{pmatrix}. \tag{4.4}$$

For any $\boldsymbol{U}\in R^n$, make the decomposition

$$\boldsymbol{U} = z\boldsymbol{q}^* + \overline{z}\,\overline{\boldsymbol{q}}^* + \boldsymbol{y}. \tag{4.5}$$

obtain

$$\begin{cases} z = \langle \boldsymbol{p}^*, \boldsymbol{U}\rangle, \\ \boldsymbol{y} = \boldsymbol{U} - \langle \boldsymbol{p}^*, \boldsymbol{U}\rangle \boldsymbol{q}^* - \langle \overline{\boldsymbol{p}}^*, \boldsymbol{U}\rangle \overline{\boldsymbol{q}}^* \end{cases} \tag{4.6}$$

In (z,y) coordinates, Equation (4.2) is

$$\begin{cases} \dot{z} = i\omega_0 z + \left\langle \boldsymbol{p}^*, \boldsymbol{F}\left(z\boldsymbol{q}^* + \overline{z}\overline{\boldsymbol{q}}^* + \boldsymbol{y}\right)\right\rangle, \\ \dot{\boldsymbol{y}} = \boldsymbol{A}\boldsymbol{y} + \boldsymbol{F}\left(z\boldsymbol{q}^* + \overline{z}\overline{\boldsymbol{q}}^* + \boldsymbol{y}\right) - \left\langle \boldsymbol{p}^*, \boldsymbol{F}\left(z\boldsymbol{q}^* + \overline{z}\overline{\boldsymbol{q}}^* + \boldsymbol{y}\right)\right\rangle \boldsymbol{q}^* \\ \qquad - \left\langle \overline{\boldsymbol{p}}^*, \boldsymbol{F}\left(z\boldsymbol{q}^* + \overline{z}\overline{\boldsymbol{q}}^* + \boldsymbol{y}\right)\right\rangle \overline{\boldsymbol{q}}^* \end{cases} \tag{4.7}$$

Using the properties of the function $\boldsymbol{B},\boldsymbol{C}$, Equation (4.7) is written as

$$\begin{cases} \dot{z} = i\omega_0 z + \frac{1}{2}\boldsymbol{G}_{20}z^2 + \boldsymbol{G}_{11}z\bar{z} + \frac{1}{2}\boldsymbol{G}_{02}\bar{z}^2 + \frac{1}{2}\boldsymbol{G}_{21}z^2\bar{z}, \\ \quad + \left\langle \boldsymbol{p}^*, \boldsymbol{B}\left(\boldsymbol{q}^*, \boldsymbol{y}\right)\right\rangle z + \left\langle \boldsymbol{p}^*, \boldsymbol{B}\left(\bar{\boldsymbol{q}}^*, \boldsymbol{y}\right)\right\rangle \bar{z} + \cdots, \\ \dot{\boldsymbol{y}} = \boldsymbol{A}\boldsymbol{y} + \frac{1}{2}\boldsymbol{H}_{20}z^2 + \boldsymbol{H}_{11}z\bar{z} + \frac{1}{2}\boldsymbol{H}_{02}\bar{z}^2 + \cdots, \end{cases} \tag{4.8}$$

where

$$\begin{aligned} &\boldsymbol{G}_{20} = \left\langle \boldsymbol{p}^*, \boldsymbol{B}\left(\boldsymbol{q}^*, \boldsymbol{q}^*\right)\right\rangle, \boldsymbol{G}_{11} = \left\langle \boldsymbol{p}^*, \boldsymbol{B}\left(\boldsymbol{q}^*, \bar{\boldsymbol{q}}^*\right)\right\rangle, \\ &\boldsymbol{G}_{02} = \left\langle \boldsymbol{p}^*, \boldsymbol{B}\left(\bar{\boldsymbol{q}}^*, \bar{\boldsymbol{q}}^*\right)\right\rangle, \boldsymbol{G}_{21} = \left\langle \boldsymbol{p}^*, \boldsymbol{C}\left(\boldsymbol{q}^*, \boldsymbol{q}^*, \bar{\boldsymbol{q}}^*\right)\right\rangle. \end{aligned} \tag{4.9}$$

$$\begin{cases} \boldsymbol{H}_{20} = \boldsymbol{B}\left(\boldsymbol{q}^*, \boldsymbol{q}^*\right) - \left\langle \boldsymbol{p}^*, \boldsymbol{B}\left(\boldsymbol{q}^*, \boldsymbol{q}^*\right)\right\rangle \boldsymbol{q}^* - \left\langle \bar{\boldsymbol{p}}^*, \boldsymbol{B}\left(\boldsymbol{q}^*, \boldsymbol{q}^*\right)\right\rangle \bar{\boldsymbol{q}}^*, \\ \boldsymbol{H}_{11} = \boldsymbol{B}\left(\boldsymbol{q}^*, \bar{\boldsymbol{q}}^*\right) - \left\langle \boldsymbol{p}^*, \boldsymbol{B}\left(\boldsymbol{q}^*, \bar{\boldsymbol{q}}^*\right)\right\rangle \boldsymbol{q}^* - \left\langle \bar{\boldsymbol{p}}^*, \boldsymbol{B}\left(\boldsymbol{q}^*, \bar{\boldsymbol{q}}^*\right)\right\rangle \bar{\boldsymbol{q}}^*, \\ \boldsymbol{H}_{02} = \boldsymbol{B}\left(\bar{\boldsymbol{q}}^*, \bar{\boldsymbol{q}}^*\right) - \left\langle \boldsymbol{p}^*, \boldsymbol{B}\left(\bar{\boldsymbol{q}}^*, \bar{\boldsymbol{q}}^*\right)\right\rangle \boldsymbol{q}^* - \left\langle \bar{\boldsymbol{p}}^*, \boldsymbol{B}\left(\bar{\boldsymbol{q}}^*, \bar{\boldsymbol{q}}^*\right)\right\rangle \bar{\boldsymbol{q}}^* \end{cases} \tag{4.10}$$

Equation (4.8) for the central manifold is given by

$$\boldsymbol{w}_{20} = \left(2i\omega_0\boldsymbol{I} - \boldsymbol{A}\right)^{-1}\boldsymbol{H}_{20}, \boldsymbol{w}_{11} = -\boldsymbol{A}^{-1}\boldsymbol{H}_{11}, \boldsymbol{w}_{02} = \left(-2i\omega_0\boldsymbol{I} - \boldsymbol{A}\right)^{-1}\boldsymbol{H}_{02}. \tag{4.11}$$

where $\boldsymbol{I}$ is a unit matrix of order n, and the simplified equation is obtained by substituting the central manifold $\boldsymbol{y} = \boldsymbol{w}z, \bar{z}$ into the first equation of Equation (4.8).

$$\begin{aligned} \dot{z} = {} & i\omega_0 z + \frac{1}{2}\boldsymbol{G}_{20}z^2 + \boldsymbol{G}_{11}z\bar{z} + \frac{1}{2}\boldsymbol{G}_{02}\bar{z}^2 \\ & + \frac{1}{2}\left\langle \boldsymbol{G}_{21} - 2\left\langle \boldsymbol{p}^*, \boldsymbol{B}\left(\boldsymbol{q}^*, \boldsymbol{A}^{-1}\boldsymbol{H}_{11}\right)\right\rangle \right. \\ & \left. + \left\langle \boldsymbol{p}^*, \boldsymbol{B}\left(\bar{\boldsymbol{q}}^*, \left(2i\omega_0\boldsymbol{I} - \boldsymbol{A}\right)^{-1}\boldsymbol{H}_{20}\right)\right\rangle \right\rangle z^2\bar{z} + \cdots \end{aligned} \tag{4.12}$$

or

$$\dot{z} = i\omega_0 z + \frac{1}{2}\boldsymbol{g}_{20}z^2 + \boldsymbol{g}_{11}z\bar{z} + \frac{1}{2}\boldsymbol{g}_{02}\bar{z}^2 + \frac{1}{2}\boldsymbol{g}_{21}z^2\bar{z} + \cdots, \tag{4.13}$$

where, $\boldsymbol{g}_{20} = \boldsymbol{G}_{20}, \boldsymbol{g}_{11} = \boldsymbol{G}_{11}, \boldsymbol{g}_{02} = \boldsymbol{G}_{02}$ and

$$\boldsymbol{g}_{21} = \boldsymbol{G}_{21} - 2\left\langle \boldsymbol{p}^*, \boldsymbol{B}\left(\boldsymbol{q}^*, \boldsymbol{A}^{-1}\boldsymbol{H}_{11}\right)\right\rangle + \left\langle \boldsymbol{p}^*, \boldsymbol{B}\left(\bar{\boldsymbol{q}}^*, \left(2i\omega_0\boldsymbol{I} - \boldsymbol{A}\right)^{-1}\boldsymbol{H}_{20}\right)\right\rangle.$$

Utilizing the following relationships

$$\boldsymbol{A}^{-1}\boldsymbol{q}^* = \frac{\boldsymbol{q}^*}{i\omega_0}, \boldsymbol{A}^{-1}\bar{\boldsymbol{q}}^* = -\frac{\bar{\boldsymbol{q}}^*}{i\omega_0}, \left(2i\omega_0\boldsymbol{I} - \boldsymbol{A}\right)^{-1}\boldsymbol{q}^* = \frac{\boldsymbol{q}^*}{i\omega_0}, \left(2i\omega_0\boldsymbol{I} - \boldsymbol{A}\right)^{-1}\bar{\boldsymbol{q}}^* = \frac{\bar{\boldsymbol{q}}^*}{3i\omega_0},$$

Reduce $\boldsymbol{g}_{21}$ to

$$\begin{aligned} \boldsymbol{g}_{21} = {} & \left\langle \boldsymbol{p}^*\boldsymbol{C}\left(\boldsymbol{q}^*, \boldsymbol{q}^*, \bar{\boldsymbol{q}}^*\right)\right\rangle - 2\left\langle \boldsymbol{p}^*, \boldsymbol{B}\left(\boldsymbol{q}^*, \boldsymbol{A}^{-1}\boldsymbol{B}\left(\boldsymbol{q}^*, \bar{\boldsymbol{q}}^*\right)\right)\right\rangle \\ & + \left\langle \boldsymbol{p}^*, \boldsymbol{B}\left(\bar{\boldsymbol{q}}^*, \left(2i\omega_0\boldsymbol{I} - \boldsymbol{A}\right)^{-1}\boldsymbol{B}\left(\boldsymbol{q}^*, \boldsymbol{q}^*\right)\right)\right\rangle \\ & + \frac{1}{i\omega_0}\left\langle \boldsymbol{p}^*, \boldsymbol{B}\left(\boldsymbol{q}^*, \boldsymbol{q}^*\right)\right\rangle\left\langle \boldsymbol{p}^*, \boldsymbol{B}\left(\boldsymbol{q}^*, \bar{\boldsymbol{q}}^*\right)\right\rangle \\ & - \frac{2}{i\omega_0}\left|\left\langle \boldsymbol{p}^*, \boldsymbol{B}\left(\boldsymbol{q}^*, \bar{\boldsymbol{q}}^*\right)\right\rangle\right|^2 - \frac{1}{3i\omega_0}\left|\left\langle \boldsymbol{p}^*, \boldsymbol{B}\left(\bar{\boldsymbol{q}}^*, \bar{\boldsymbol{q}}^*\right)\right\rangle\right|^2. \end{aligned} \tag{4.14}$$

We obtain the formula for the first *Lyapunov* coefficient as follows

$$l_1(0)=\frac{1}{2\omega_0}Re\left\{\left\langle \boldsymbol{p}^*,\boldsymbol{C}\left(\boldsymbol{q}^*,\boldsymbol{q}^*,\bar{\boldsymbol{q}}^*\right)\right\rangle-2\left\langle \boldsymbol{p}^*,\boldsymbol{B}\left(\boldsymbol{q}^*,\boldsymbol{A}^{-1}\boldsymbol{B}\left(\boldsymbol{q}^*,\bar{\boldsymbol{q}}^*\right)\right)\right\rangle \right.$$
$$\left.+\left\langle \boldsymbol{p}^*\boldsymbol{B}\left(\bar{\boldsymbol{q}}^*,\left(2i\omega_0\boldsymbol{I}_4-\boldsymbol{A}\right)^{-1}\boldsymbol{B}\left(\boldsymbol{q}^*,\boldsymbol{q}^*\right)\right)\right\rangle\right\} \tag{4.15}$$

where

$$\boldsymbol{A}=\boldsymbol{J}_E^*$$

Based on the expression in Equation (4.5), we can compute

$$\boldsymbol{B}\left(\boldsymbol{q}^*,\boldsymbol{q}^*\right)=\begin{pmatrix}\dfrac{2\left[\left(e+i\omega_0\right)\left(h+i\omega_0\right)\right]\left[\left(1+my^*+i\omega_0\right)\left(e+i\omega_0\right)\left(h+i\omega_0\right)-n\right]}{x^*}\\ \dfrac{2c\left(h+i\omega_0\right)^2\left[\left(1+w^*\right)\left(e+i\omega_0\right)-x^*\right]}{\left(1+w^*\right)^3}\\ 0\\ 0\end{pmatrix}$$

$$\boldsymbol{B}\left(\boldsymbol{q}^*,\bar{\boldsymbol{q}}^*\right)=\begin{pmatrix}\dfrac{\left(e+i\omega_0\right)\left(h+i\omega_0\right)\left[\left(1+my^*-i\omega_0\right)\left(e-i\omega_0\right)\left(h-i\omega_0\right)-n\right]}{x^*}\\ +\dfrac{\left(e-i\omega_0\right)\left(h-i\omega_0\right)\left[\left(1+my^*+i\omega_0\right)\left(e+i\omega_0\right)\left(h+i\omega_0\right)-n\right]}{x^*}\\ \dfrac{2c\left(h^2+\omega_0^2\right)\left[e\left(1+w^*\right)-x^*\right]}{\left(1+w^*\right)^3}\\ 0\\ 0\end{pmatrix}$$

$$\boldsymbol{A}^{-1}=\frac{1}{\eta}\begin{pmatrix}A_{11}&A_{12}&A_{13}&A_{14}\\A_{21}&A_{22}&A_{23}&A_{24}\\A_{31}&A_{32}&A_{33}&A_{34}\\A_{41}&A_{42}&A_{43}&A_{44}\end{pmatrix},\quad \left(2i\omega_0\boldsymbol{I}_4-\boldsymbol{A}\right)^{-1}=\frac{1}{\theta}\begin{pmatrix}B_{11}&B_{12}&B_{13}&B_{14}\\B_{21}&B_{22}&B_{23}&B_{24}\\B_{31}&B_{32}&B_{33}&B_{34}\\B_{41}&B_{42}&B_{43}&B_{44}\end{pmatrix}$$

where

$$\eta=h\left[\left(1+my^*\right)de+\frac{mc\left(x^*\right)^2}{\left(1+w^*\right)^2}+mex^*\left(\frac{cw^*}{1+w^*}+1\right)\right]-nd$$

$$\theta=\left(2i\omega_0+h\right)\left[\left(1+my^*+2i\omega_0\right)\left(2i\omega_0+d\right)\left(2i\omega_0+e\right)+\frac{mc\left(x^*\right)^2}{\left(1+w^*\right)^2}\right.$$
$$\left.+mx^*\left(2i\omega_0+e\right)\left(\frac{cw^*}{1+w^*}+1\right)\right]-n\left(2i\omega_0+d\right)$$

$$A_{11}=-deh,A_{12}=-\left[\left(\frac{cw^*}{1+w^*}+1\right)eh+\frac{cx^*h}{\left(1+w^*\right)^2}\right],A_{13}=dh,A_{14}=-d,$$

$$A_{21}=mehx^*, A_{22}=n-\left(1+my^*\right)eh, A_{23}=mhx^*, A_{24}=mx^*,$$

$$A_{31}=\frac{mch\left(x^*\right)^2}{\left(1+w^*\right)^2}-nd, A_{32}=-\left[\left(1+my^*\right)h\frac{cx^*}{\left(1+w^*\right)^2}+n\left(\frac{cw^*}{1+w^*}+1\right)\right],$$

$$A_{33}=-\left[\left(1+my^*\right)dh+mhx^*\left(\frac{cw^*}{1+w^*}+1\right)\right], A_{34}=-\left[\left(1+my^*\right)d+mx^*\left(\frac{cw^*}{1+w^*}+1\right)\right]$$

$$A_{41}=-ned, A_{42}=-\left[ne\left(\frac{cw^*}{1+w^*}+1\right)+n\frac{cx^*}{\left(1+w^*\right)^2}\right], A_{43}=-nd,$$

$$A_{44}=-\left[\left(1+my^*\right)de+\frac{mc\left(x^*\right)^2}{\left(1+w^*\right)^2}+mex^*\left(\frac{cw^*}{1+w^*}+1\right)\right],$$

$$B_{11}=\left(2i\omega_0+d\right)\left(2i\omega_0+e\right)\left(2i\omega_0+h\right),$$

$$B_{12}=\left(1+my^*+2i\omega_0\right)\left(2i\omega_0+h\right)\left(2i\omega_0+e\right)+\frac{cx^*\left(2i\omega_0+h\right)}{\left(1+w^*\right)^2},$$

$$B_{13}=\left(2i\omega_0+d\right)\left(2i\omega_0+h\right), B_{14}=\left(2i\omega_0+d\right), B_{21}=-mx^*\left(2i\omega_0+e\right)\left(2i\omega_0+h\right),$$

$$B_{22}=\left(1+my^*+2i\omega_0\right)\left(2i\omega_0+h\right)\left(2i\omega_0+e\right)-n, B_{23}=-mx^*\left(2i\omega_0+h\right),$$

$$B_{24}=-mx^*, B_{31}=\left(2i\omega_0+d\right)n-\frac{mc\left(x^*\right)^2\left(2i\omega_0+h\right)}{\left(1+w^*\right)^2},$$

$$B_{32}=\left(1+my^*+2i\omega_0\right)\left(2i\omega_0+h\right)\frac{cx^*}{\left(1+w^*\right)^2}+n\left(\frac{cw^*}{1+w^*}+1\right),$$

$$B_{33}=\left(1+my^*+2i\omega_0\right)\left(2i\omega_0+d\right)\left(2i\omega_0+h\right)+mx^*\left(2i\omega_0+h\right)\left(\frac{cw^*}{1+w^*}+1\right),$$

$$B_{34}=\left(1+my^*+2i\omega_0\right)\left(2i\omega_0+d\right)mx^*\left(\frac{cw^*}{1+w^*}+1\right), B_{41}=n\left(2i\omega_0+d\right)\left(2i\omega_0+e\right),$$

$$B_{42}=n\left(2i\omega_0+e\right)\left(\frac{cw^*}{1+w^*}+1\right)+n\frac{cx^*}{\left(1+w^*\right)^2}, B_{43}=n\left(2i\omega_0+d\right),$$

$$B_{44}=\left(1+my^*+2i\omega_0\right)\left(2i\omega_0+d\right)\left(2i\omega_0+e\right)+\frac{mc\left(x^*\right)^2}{\left(1+w^*\right)^2}+mx^*\left(2i\omega_0+e\right)\left(\frac{cw^*}{1+w^*}+1\right).$$

command $\boldsymbol{B}\left(\boldsymbol{q}^*,\overline{\boldsymbol{q}}^*\right)=\left(r_1,r_2,0,0\right)^{\mathrm{T}}$

then

$$\boldsymbol{\mu}_{11}=-\boldsymbol{A}^{-1}\boldsymbol{B}\left(\boldsymbol{q}^*,\overline{\boldsymbol{q}}^*\right)=-\frac{1}{\eta}\begin{pmatrix}A_{11}r_1+A_{12}r_2\\A_{21}r_1+A_{22}r_2\\A_{31}r_1+A_{32}r_2\\A_{41}r_1+A_{42}r_2\end{pmatrix}$$

command $\boldsymbol{B}\left(\boldsymbol{q}^*,\boldsymbol{q}^*\right)=\left(v_1,v_2,0,0\right)^{\mathrm{T}}$

then

$$\boldsymbol{\mu}_{20}=\left(2i\omega_0-\boldsymbol{A}\right)^{-1}\boldsymbol{B}\left(\boldsymbol{q}^*,\boldsymbol{q}^*\right)=\frac{1}{\theta}\begin{pmatrix}B_{11}v_1+B_{12}v_2\\B_{21}v_1+B_{22}v_2\\B_{31}v_1+B_{32}v_2\\B_{41}v_1+B_{42}v_2\end{pmatrix}$$

command $q=\left(q_{11},q_{21},q_{31},1\right)^{\mathrm{T}}, p=\left(p_{11},p_{21},p_{31},1\right)^{\mathrm{T}}$

therefore

$$\boldsymbol{B}\left(\boldsymbol{q}^*,-\mu_{11}\right)=\begin{pmatrix}\dfrac{-m\left[q_{11}\left(A_{21}r_1+A_{22}r_2\right)+q_{21}\left(A_{11}r_1+A_{12}r_2\right)\right]}{\eta}\\\dfrac{c\left(1+w^*\right)\left[q_{11}\left(A_{31}r_1+A_{32}r_2\right)+q_{31}\left(A_{11}r_1+A_{12}r_2\right)\right]-2cx^*q_{31}\left(A_{31}r_1+A_{32}r_2\right)}{\eta\left(1+w^*\right)^3}\\0\\0\end{pmatrix}$$

therefore

$$\left\langle p,B\left(\boldsymbol{q}^*,-\boldsymbol{\mu}_{11}\right)\right\rangle=\frac{mp_{11}\left[q_{11}\left(A_{21}r_1+A_{22}r_2\right)+q_{21}\left(A_{11}r_1+A_{12}r_2\right)\right]}{\eta}$$
$$-\frac{cp_{21}\left(1+w^*\right)\left[q_{11}\left(A_{31}r_1+A_{32}r_2\right)+q_{31}\left(A_{11}r_1+A_{12}r_2\right)\right]-2cx^*p_{21}q_{31}\left(A_{31}r_1+A_{32}r_2\right)}{\eta\left(1+w^*\right)^3}$$

note $\left\langle p,B\left(\boldsymbol{q}^*,-\boldsymbol{\mu}_{11}\right)\right\rangle=M_1$

command $q=\left(\overline{q_{11}},q_{21},\overline{q_{31}},1\right)^{\mathrm{T}}$

therefore

$$\boldsymbol{B}\left(\overline{q}^*,-\mu_{20}\right)=\begin{pmatrix}\dfrac{-m\left[\overline{q_{11}}\left(A_{21}r_1+A_{22}r_2\right)+\overline{q_{21}}\left(A_{11}r_1+A_{12}r_2\right)\right]}{\theta}\\\dfrac{c\left(1+w^*\right)\left[\overline{q_{11}}\left(A_{31}r_1+A_{32}r_2\right)+\overline{q_{31}}\left(A_{11}r_1+A_{12}r_2\right)\right]-2cx^*\overline{q_{31}}\left(A_{31}r_1+A_{32}r_2\right)}{\theta\left(1+w^*\right)^3}\\0\\0\end{pmatrix}$$

therefore

$$\left\langle p,B\left(\overline{q}^*,-\mu_{20}\right)\right\rangle=\frac{-mp_{11}\left[\overline{q_{11}}\left(A_{21}r_1+A_{22}r_2\right)+\overline{q_{21}}\left(A_{11}r_1+A_{12}r_2\right)\right]}{\theta}$$
$$+\frac{cp_{21}\left(1+w^*\right)\left[\overline{q_{11}}\left(A_{31}r_1+A_{32}r_2\right)+\overline{q_{31}}\left(A_{11}r_1+A_{12}r_2\right)\right]-2cx^*p_{21}\overline{q_{31}}\left(A_{31}r_1+A_{32}r_2\right)}{\theta\left(1+w^*\right)^3}$$

note $\left\langle p,B\left(\overline{q}^*,-\mu_{20}\right)\right\rangle=M_2$

$$\boldsymbol{C}\left(\boldsymbol{q}^*,\boldsymbol{q}^*,\overline{\boldsymbol{q}}^*\right)=\begin{pmatrix}0\\\dfrac{6cx^*q_{31}^2\overline{q_{31}}-2c\left(1+w^*\right)\left(2q_{11}q_{31}\overline{q_{31}}\right)+q_{31}^2\overline{q_{11}}}{\left(1+w^*\right)^4}\\0\\0\end{pmatrix}$$

therefore

$$\left\langle p, C\left(\boldsymbol{q}^*, \boldsymbol{q}^*, \overline{\boldsymbol{q}}^*\right)\right\rangle = \frac{p_{21}\left[6cx^* q_{31}^2 \overline{q_{31}} - 2c\left(1+w^*\right)\left(2q_{11}q_{31}\overline{q_{31}}\right) + q_{31}^2\overline{q_{11}}\right]}{\left(1+w^*\right)^4}$$

note $\left\langle p, C\left(\boldsymbol{q}^*, \boldsymbol{q}^*, \overline{\boldsymbol{q}}^*\right)\right\rangle = M_3$

Therefore, the first *Lyapunov* coefficients are

$$\begin{aligned} l_1(0) &= \frac{1}{2\omega_0} Re\left\{\left\langle \boldsymbol{p}^*, \boldsymbol{C}\left(\boldsymbol{q}^*, \boldsymbol{q}^*, \overline{\boldsymbol{q}}^*\right)\right\rangle - 2\left\langle \boldsymbol{p}^*, \boldsymbol{B}\left(\boldsymbol{q}^*, -\boldsymbol{\mu}_{11}\right)\right\rangle \right. \\ &\quad \left. + \left\langle \boldsymbol{p}^*, \boldsymbol{B}\left(\overline{\boldsymbol{q}}^*, -\boldsymbol{\mu}_{20}\right)\right\rangle\right\} \\ &= \frac{1}{2\omega_0} Re\left[M_3 - 2M_1 + M_2\right] \end{aligned}$$

When $l_1(n) < 0$, the *Hopf* bifurcation occurring at the equilibrium point $E^* = \left(x^*, y^*, w^*, z^*\right)$ is a subcritical bifurcation, and stable periodic trajectories arise at $n - n_0 > 0$.

When $l_1(n) > 0$, the *Hopf* bifurcation occurring at the equilibrium point $E^* = \left(x^*, y^*, w^*, z^*\right)$ is a subcritical bifurcation, and stable periodic trajectories arise at $n - n_0 < 0$.

5. Numerical Simulation

Select the first set of parameters

$$e = 0.03; h = 0.5; n = 0.016; m = 0.1; d = 0.01; c = 0.4.$$

The positive equilibrium point at this point is

$$E^* = (0.006237239314, 0.6666666666, 0.2079079772, 0.4158159543)$$

$$n - eh = 0.001 > 0.$$

A positive equilibrium exists when this condition is satisfied. This moment

$$a_1 = h + d + e + (m \cdot y) + 1; a_2 = dmy + emy + hmy + de + dh + eh + mx + d + e + h;$$

$$a_3 = demy + dhmy + ehmy + deh + emx + hmx + de + dh + eh - n;$$

$$a_4 = dehmy + ehmx + deh - dn;$$

$$b_1 = \frac{cmx^*}{1+w^*}; b_2 = \frac{cmx^{*2}}{\left(1+w^*\right)^2} + \frac{cmhx^* w^*}{1+w^*} + \frac{cmex^* w^*}{1+w^*}; b_3 = \frac{cmhx^{*2}}{\left(1+w^*\right)^2} + \frac{cmehx^* w^*}{1+w^*};$$

$$A_1 = 1 + e + h; A_2 = eh + e + h; A_3 = eh - n.$$

$$B_1 = a_1; B_2 = a_2 + b_1; B_3 = a_3 + a_2; B_4 = a_4 + b_3;$$

$$A_1 = 1.53; A_2 = 0.545; A_3 = -0.001$$

$$B_1 = 1.606666667; B_2 := 0.5971302709;$$
$$B_3 = 0.00615773321; B_4 = 0.00001053326995.$$

$$\Delta_1 = 1.606666667 > 0, \Delta_2 = 0.9532315689 > 0, \Delta_3 = 0.005842555344 > 0.$$

Thus, the ordinary equilibrium of the system (1.3) $E_0 = (0,0,0,0)$. It's unstable, positive equilibrium

$$E^* = (0.006237239314, 0.6666666666, 0.2079079772, 0.4158159543)$$

is locally asymptotically stable.

At this equilibrium,

$$\Delta_3 = 0.005842555344 \approx 0, Re\left(\frac{\partial_\lambda}{\partial_n}(n_0)\right) = 0.8022644210 > 0$$

By calculating

$$\boldsymbol{q}^* = \begin{pmatrix} 0.01116738597 + 0.03281129808 \times i \\ 9.811082689 - 57.22094010 \times i \\ 0.5 + 0.06190810959 \times i \\ 1 \end{pmatrix},$$

$$\boldsymbol{p}^* = \begin{pmatrix} 31.25000000 - 3.869256849 \times i \\ -0.09912680315 - 0.6136752992 \times i \\ 148.7629882 + 418.8597641 \times i \\ 1 \end{pmatrix}$$

$$\boldsymbol{B}\left(\boldsymbol{q}^*, \boldsymbol{q}^*\right) = \begin{pmatrix} -0.3974114938 + 0.06341879298 \times i \\ 0.001250837561 + 0.009199094398 \times i \\ 0 \\ 0 \end{pmatrix},$$

$$\boldsymbol{B}\left(\boldsymbol{q}^*, \overline{\boldsymbol{q}}^*\right) = \begin{pmatrix} 1.967230225 - 5.356640473 \times i \\ 0.003456663596 \\ 0 \\ 0 \end{pmatrix}$$

$$\boldsymbol{C}\left(\boldsymbol{q}^*, \boldsymbol{q}^*, \overline{\boldsymbol{q}}^*\right) = \begin{pmatrix} -0.4530370791 + 0.0001105002389 \times i \\ 0 \\ 0 \\ 0 \end{pmatrix}.$$

obtained further

$$\left\langle \boldsymbol{p}^*, \boldsymbol{C}\left(\boldsymbol{q}^*, \boldsymbol{q}^*, \overline{\boldsymbol{q}}^*\right)\right\rangle = -0.00001455511715 + 5.511091162 \times 10^{-6} \times i,$$

$$\left\langle p, B\left(q, -\mu_{11}\right)\right\rangle = -57.54924740 + 35.89973285 \times i,$$

$$\left\langle p, B\left(\overline{q}, -\mu_{20}\right)\right\rangle = -0.004036548250 + 0.001089961508 \times i,$$

Bringing in the above results gives $l_1(0) = 929.5586995 > 0$. By the *Hopf* bifurcation direction and the stability theorem for periodic solutions we know that when

$$Re\left(\frac{\partial_\lambda}{\partial_n}(n_0)\right) = 0.8022644210 > 0$$

$l_1(0) = 929.5586995 > 0$. The direction of the resulting *Hopf* bifurcation is then supercritical and the periodic solution is stabilized.

Select the second set of parameters

$$e = 0.1; h = 0.4; n = 0.05; m = 0.01; d = 0.18; c = 3.$$

The positive equilibrium point at this point is

$$E^* = (1.194204936, 25.00000000, 11.94204936, 29.85512340)$$

$$n - eh = 0.01 > 0.$$

A positive equilibrium exists when this condition is satisfied. this moment

$$a_1 = h + d + e + (m \cdot y) + 1; a_2 = dmy + emy + hmy + de + dh + eh + mx + d + e + h;$$

$$a_3 = demy + dhmy + ehmy + deh + emx + hmx + de + dh + eh - n;$$

$$a_4 = dehmy + ehmx + deh - dn;$$

$$b_1 = \frac{cmx^*}{1+w^*}; b_2 = \frac{cmx^{*2}}{(1+w^*)^2} + \frac{cmhx^*w^*}{1+w^*} + \frac{cmex^*w^*}{1+w^*}; b_3 = \frac{cmhx^{*2}}{(1+w^*)^2} + \frac{cmehx^*w^*}{1+w^*};$$

$$A_1 = 1 + e + h; A_2 = eh + e + h; A_3 = eh - n.$$

$$B_1 = a_1; B_2 = a_2 + b_1; B_3 = a_3 + a_2; B_4 = a_4 + b_3;$$

$$A_1 = 1.5; A_2 = 0.54; A_3 = -0.01$$

$$B_1 = 1.930000000; B_2 := 0.9947102469;$$

$$B_3 = 0.1424554306; B_4 = 0.001902172228.$$

$$\Delta_1 = 1.930000000 > 0, \Delta_2 = 1.777335346 > 0, \Delta_3 = 0.2461056707 > 0.$$

Thus, the ordinary equilibrium point

$$E_0 = (0, 0, 0, 0)$$

of the system (1.3) is unstable, and the positive equilibrium point

$$E^* = (1.194204936, 25.00000000, 11.94204936, 29.85512340)$$

is locally asymptotically stable. At this equilibrium,

$$\Delta_3 = 0.2461056707 \approx 0, Re\left(\frac{\partial_\lambda}{\partial_n}(n_0)\right) = 0.2517327382 > 0$$

By calculating

$$\boldsymbol{q}^* = \begin{pmatrix} -0.03381110396 + 0.1358409952 \times i \\ 10.81635388 - 13.44956558 \times i \\ 0.4 + 0.2716819905 \times i \\ 1 \end{pmatrix},$$

$$\boldsymbol{p}^* = \begin{pmatrix} 8.000000000 - 5.433639810 \times i \\ -0.4047729107 - 0.6109417226 \times i \\ 4.123727214 + 1.017145980 \times i \\ 1 \end{pmatrix}$$

$$\boldsymbol{B}(\boldsymbol{q}^*, \boldsymbol{q}^*) = \begin{pmatrix} -0.02922579018 - 0.03848097872 \times i \\ -0.002091370516 + 0.0008989557992 \times i \\ 0 \\ 0 \end{pmatrix},$$

$$\boldsymbol{B}(\boldsymbol{q}^*, \overline{\boldsymbol{q}}^*) = \begin{pmatrix} -0.006385495580 - 0.1238957500 \times i \\ 0.00006471533850 \\ 0 \\ 0 \end{pmatrix}$$

$$\boldsymbol{C}\left(\boldsymbol{q}^*,\boldsymbol{q}^*,\overline{\boldsymbol{q}}^*\right)=\begin{pmatrix}-0.002696189162+0.00004867042542\times i\\0\\0\\0\end{pmatrix}.$$

obtained further

$$\left\langle \boldsymbol{p}^*,\boldsymbol{C}\left(\boldsymbol{q}^*,\boldsymbol{q}^*,\overline{\boldsymbol{q}}^*\right)\right\rangle = 8.317489373\times10^{-6}-8.132167325\times10^{-7}\times i,$$

$$\left\langle p,B\left(q,-\mu_{11}\right)\right\rangle = 0.001378750347-0.1048477482\times i,$$

$$\left\langle p,B\left(\overline{q},-\mu_{20}\right)\right\rangle = 0.001922033460-0.00272496253\times i,$$

Bringing in the above results gives $l_1(0)=-0.001522275628<0$. By the *Hopf* bifurcation direction and the stability theorem for periodic solutions we know that when

$$Re\left(\frac{\partial_\lambda}{\partial_n}\left(n_0\right)\right)=0.8022644210>0$$

$l_1(0)=-0.001522275628<0$. The direction of the resulting *Hopf* bifurcation is subcritical and the periodic solution is unstable.

Figure 1 shows the solution curve for parameter values

$$e=0.2;h=0.55;n=3;m=0.2;d=0.007;c=0.8.$$

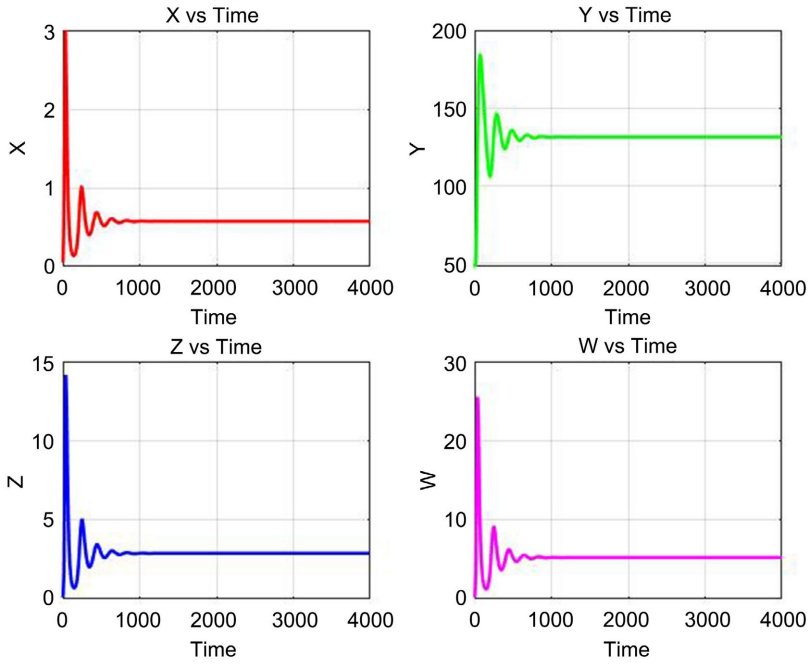

Figure 1. The solution curve when n equals 3.

The solution curve changes from unstable to stable.

Figure 2 shows the solution curve for parameter values

$$e=0.2;h=0.55;n=0.2;m=0.2;d=0.007;c=0.8.$$

The curve produces an oscillatory behavior, and the solution curve has been in

an unstable state.

Figure 3 shows the limit ring for parameter values

$$e = 0.2; h = 0.55; n = 0.2; m = 0.2; d = 0.007; c = 0.8.$$

it can be seen that the solution curves are unstable under this set of parameters, and there are *Hopf* branching cycle solutions.

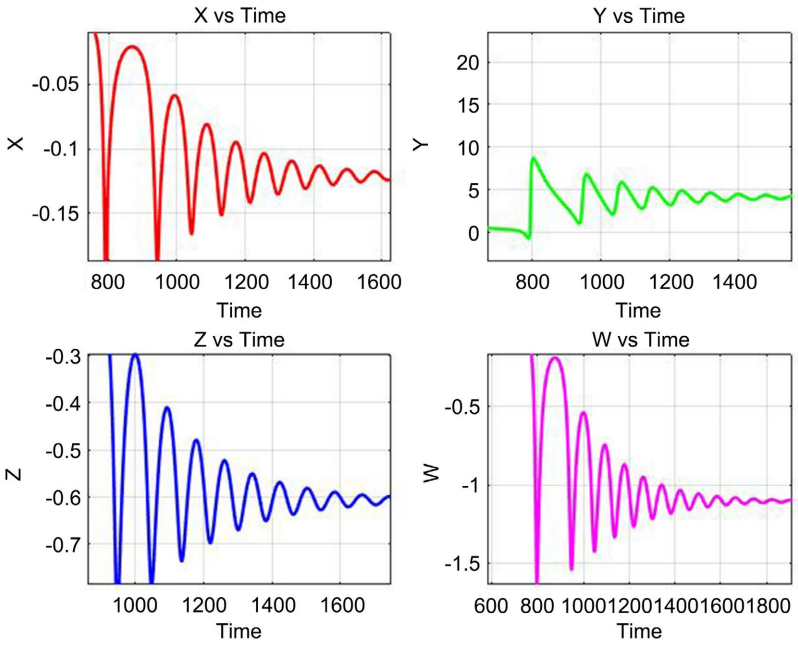

Figure 2. The solution curve when n equals 0.2.

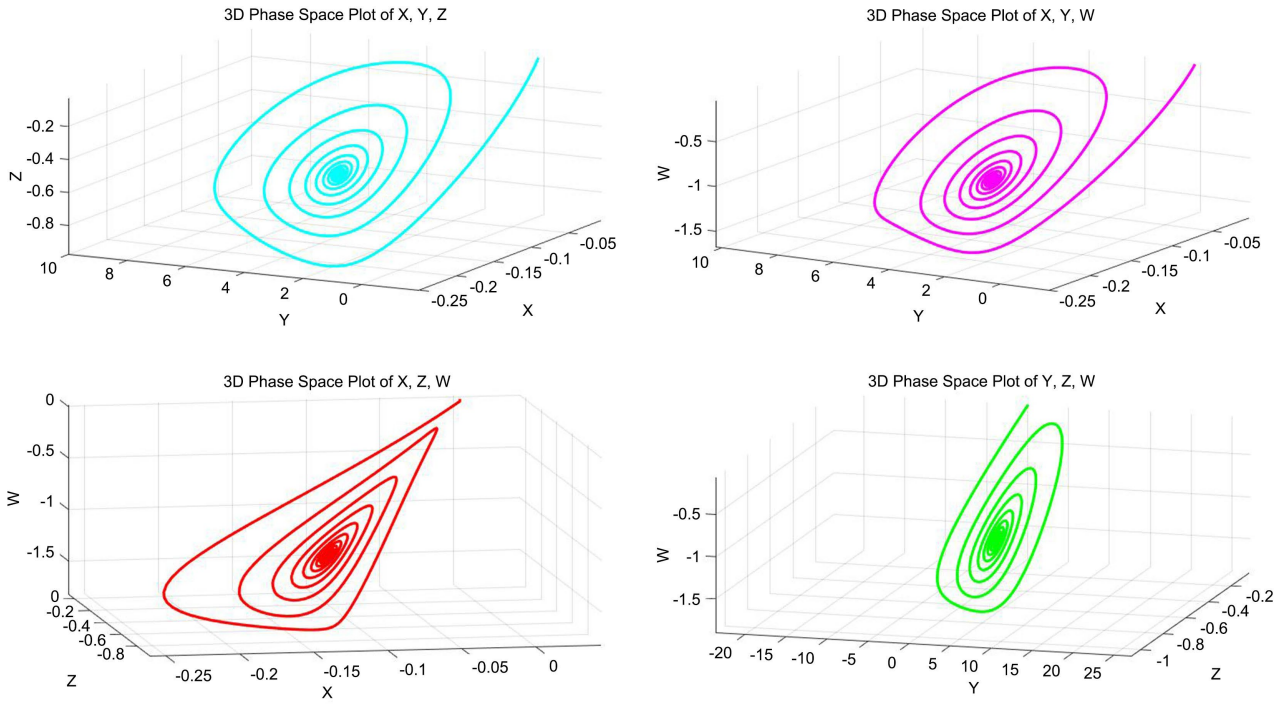

Figure 3. Limit circle.

Next, we will compare the advantages and disadvantages of the model with and without the saturated functional reaction in the numerical simulation section. The model without the saturated functional reaction is the second equation in Equation (1.3) with the denominator removed, so we will not write the specific equation here.

We next examine the advantages and disadvantages of the ability to predict multiple sclerosis between the two models by adjusting the values of some of the parameters in the first set of parameters of the numerical simulation.

Select the first set of parameters

$$e=0.03; h=0.5; n=0.016; m=0.1; d=0.01; c=0.4.$$

The equilibrium of the original model is

$$H^{*}=\left(9.998675002\times10^{-6}, 0.6666666666, 0.0003332891668, 0.0006665783335\right)$$

The positive equilibrium point at this point is

$$E^{*}=\left(0.006237239314, 0.6666666666, 0.2079079772, 0.4158159543\right)$$

This equilibrium point can be interpreted as the number of individual cells at this set of parameter values.

Next, we will transform some of the parameters to test the predictive ability of the two for disease.

First, we increase the value of the parameter c, which is a composite representation of the rate of Treg in PAPC-activated Teff and PAPC-activated Treg. We can get

$$e=0.03; h=0.5; n=0.016; m=0.1; d=0.01; c=100.$$

The equilibrium of the original model is

$$H^{*}=\left(9.687194198\times10^{-6}, 0.6666666666, 0.0003229064732, 0.0006458129465\right)$$

The positive equilibrium point at this point is

$$E^{*}=\left(0.001296416541, 0.6666666666, 0.04321388470, 0.08642776940\right)$$

By increasing the value of parameter c we can find that at this time the value of regulatory T cells did not change in both models, but the value of effector T cells in the model after the addition of saturated functional response did decrease dramatically, whereas the value of effector T cells in the original model was almost unchanged, which is in line with the inhibition of multiple sclerosis, *i.e.* the regulatory T cells are positive feedback, and the effector T cells are negative feedback, which is to say that when regulatory T cells remain unchanged, the number of effector T cells decreases dramatically. This suggests that the addition of a saturating functional response can inhibit the onset of multiple sclerosis and make it easier to predict the onset of multiple sclerosis.

For the second test, we intended to increase the values of the parameters n and e, n representing the rate of antigen uptake by immature PAPCs and e representing the rate of apoptosis of effector T cells.

$$e=30; h=0.5; n=16; m=0.1; d=0.01; c=0.4.$$

The equilibrium of the original model is

$$H^* = (0.009998675002, 0.6666666666, 0.0003332891668, 0.0006665783335)$$

The positive equilibrium point at this point is

$$E^* = (0.006666073810, 0.6666666666, 0.0002222024604, 0.0004444049207)$$

This time, we will briefly explain the results. The original model is the same as the model with the functional response added, the number of regulatory T cells is still unchanged, and there is no change in the number of effector T cells in the original model at this time. In the original model, there is no change in the number of effector T cells, and the number of effector T cells in the original model does not change at all. However, the number of effector T cells in the model with the addition of the functional response decreases dramatically, and the model with the addition of the functional response has a better prediction effect in this case.

$$e = 0.03; h = 0.5; n = 0.016; m = 0.5; d = 0.01; c = 0.4.$$

The equilibrium of the original model is

$$H^* = (9.998675002 \times 10^{-6}, 0.1333333333, 0.0003332891668, 0.0006665783335)$$

The positive equilibrium point at this point is

$$E^* = (0.001311364605, 0.1333333333, 0.04371215350, 0.08742430700)$$

For the last test, we intend to increase the value of the parameter m, which is the compound rate of PAPC inhibition by Treg and the rate of PAPC inhibition by other cells. At this point, the number of effector T cells decreased by the same amount, but the number of effector T cells decreased significantly in the model with the addition of functional response. Based on the results of the first set of data, it is reasonable to assume that the prediction of multiple sclerosis is still better with the addition of functional response in this set of parameter tests.

6. Conclusions

In this paper, we delve into a class of multiple sclerosis models distinguished by their saturated functional responses, wherein the system (1.3) invariably possesses a normal equilibrium point $E_0(0,0,0,0)$. The article proceeds to scrutinize the prerequisites for the existence of a normal numerical equilibrium point within this model. Furthermore, it conducts an in-depth examination of the system's stability at both the normal and positive equilibrium points. The findings indicate that the system's positive equilibrium point attains local asymptotic stability when the condition $n > e * h$. Additionally, when the rate of antigen uptake by immature specialized antigen-presenting cells, denoted as n, is designated as the bifurcation parameter and incremented to a critical threshold n_0, the system (1.3) undergoes a *Hopf* bifurcation in the vicinity of the positive equilibrium point E^*.

The mechanism underlying relapses in multiple sclerosis [16] is multifaceted, with the conventional wisdom positing a defective negative feedback loop between effector T cells and regulatory T cells as one of the instigating factors. However,

our study uncovers that augmenting the activation rate of specialized antigen-presenting cells or intensifying the auto-reactive T cell-induced damage may elevate the risk of relapses in multiple sclerosis. This discovery sheds light on the underlying factors that potentiate positive feedback loops between specialized antigen-presenting cells and auto-reactive effector T cells, thereby opening up novel avenues for mitigating relapses in this condition. With an enhanced comprehension of the effector T cell mechanism, more precise predictions of multiple sclerosis relapses can be anticipated in the foreseeable future.

The incorporation of the saturating functional response transformed the system from linear to nonlinear, resulting in a change where the growth rate of regulatory T cells was no longer directly proportional to the increase in specialized antigen-presenting cells. Instead, it became a saturating function influenced by both effector T cells and specialized antigen-presenting cells. When the count of effector T cells decreased, the growth rate of regulatory T cells gradually increased, offering improved prediction capabilities for relapses in multiple sclerosis. This gradual increase in regulatory T cell growth, as effector T cell numbers decline, more effectively inhibits relapses of multiple sclerosis, highlighting the saturation effect in the interaction dynamics among these three components. In the saturation function $f(A,E)=\frac{aEA}{1+bE}$, the term 1 serves as a measure of saturation degree, facilitating a simpler calculation process. This reflects the phenomenon where an increase in effector T cells leads to a gradual slowdown in the growth rate of regulatory T cells.

By incorporating a saturating functional response, the system achieved enhanced accuracy in modeling the interactions between mature antigen-presenting cells (PAPCs) and effector T cells (Teff) [17], as well as other cellular components. These interactions encompass antigen presentation, signaling cascades, cellular proliferation, and differentiation. In particular, the saturated functional response function elucidates how mature PAPC modulates its antigen presentation efficiency and signaling patterns in response to the quantity and activity of Teff cells. These adaptive adjustments are crucial for maintaining the equilibrium and stability of the immune system, thereby averting both excessive and inadequate immune responses. Concurrently, regulatory T cells (Treg) play a pivotal role within this system. They exert inhibitory effects on the proliferation and activity of effector T cells (Teff), thereby hindering the initiation and progression of autoimmune disorders. This suppressive function may entail direct cell-to-cell interactions, the secretion of inhibitory cytokines, and additional mechanisms.

With the addition of saturated functional responses, the model was able to better predict the onset of multiple sclerosis [18] for the following reasons:

1) More refined modeling of biological processes

While the original model was able to describe some of the basic kinetic processes in multiple sclerosis, it failed to adequately account for the complexity of cell-cell interactions. The introduction of a saturated functional response function simulates the nonlinear inhibitory effect of mature, dedicated antigen-presenting

cells (PAPCs) on antigen-presenting processes (especially on antigen presentation to T cells). This inhibitory effect is crucial in the pathologic process of multiple sclerosis.

2) Embodiment of nonlinear inhibition

In multiple sclerosis, excessive antigen presentation may exacerbate the immune response and lead to tissue damage. The saturated functional response allows the model to more accurately reflect this nonlinear relationship by adjusting the degree of inhibition of antigen-presenting cells by PAPC cells. As the number of PAPC cells increases, their inhibitory effect on antigen-presenting cells is enhanced, thereby reducing effective antigen presentation.

According to the saturation-type functional response function, the inhibitory effect of PAPC cells on antigen-presenting cells was significant at this time, resulting in a decrease in the effective presentation of antigen. This reduction may have reduced the overreaction of the immune system and thus slowed down the development of multiple sclerosis to some extent.

In contrast, in the original model, this slowing effect may not be accurately predicted because this nonlinear inhibitory effect was not considered.

Analysis:

With the addition of the saturated functional response, the model improves the accuracy of its prediction of the onset and progression of multiple sclerosis by introducing more complex biological processes (particularly nonlinear interactions between cells. This improvement allows the model to more fully reflect key factors in the pathologic process of the disease, thereby providing more effective guidance for disease treatment and prevention.

The shortcomings of this model are also very obvious. Although the ability of this model to predict the occurrence of multiple sclerosis has been improved with the addition of the saturation function response compared with the original model, the accuracy of its prediction still needs to be improved, especially the failure to test its feasibility and accuracy by using some statistically related expertise, such as sensitivity analyses and parameter estimation, etc. It is hoped that this model can be tested by statistically related methods in the future. It is hoped that more accurate tests can be carried out by statistical methods rather than purely mathematical methods.

By incorporating saturated functional responses, the four-dimensional dynamical system not only simulates the interactions among immune cells in the multiple sclerosis model with greater precision, but also enhances our comprehension of the immune system's functionalities and regulatory mechanisms. This discovery unveils the intricate and sophisticated nature of cell-cell interactions within the immune system, elucidating how these interactions collectively maintain their balance and stability. This insight holds significant implications for our understanding of autoimmune disease pathogenesis and the development of novel therapies and medications. For instance, by modulating the interplay between mature PAPC and effector T cells (Teff) as well as regulatory T cells (Treg) [19] [20], new

therapeutic approaches for autoimmune diseases, such as multiple sclerosis, may be devised. These therapies could encompass adjusting antigen-presenting efficiency, suppressing effector T cells (Teff) activity, and augmenting regulatory T cells (Treg) function, ultimately leading to improved treatment outcomes and a better quality of life for patients.

Conflicts of Interest

The author declares no conflicts of interest regarding the publication of this paper.

References

[1] Kumar, B.V., Connors, T.J. and Farber, D.L. (2018) Human T Cell Development, Localization, and Function Throughout Life. *Immunity*, **48**, 202-213. https://doi.org/10.1016/j.immuni.2018.01.007

[2] Murphy, K. and Weaver, C. (2016) Janeway's Immunobiology. Garland Science.

[3] Janeway, C.A., Travers, P., Walport, M. and Shlomchik, M.J. (2005) Immunobiology: The Immune System in Health and Disease. 6th Edition, Garland.

[4] Grigoriadis, N. and van Pesch, V. (2015) A Basic Overview of Multiple Sclerosis Immunopathology. *European Journal of Neurology*, **22**, 3-13. https://doi.org/10.1111/ene.12798

[5] Weatherley, G., Araujo, R.P., Dando, S.J. and Jenner, A.L. (2023) Could Mathematics Be the Key to Unlocking the Mysteries of Multiple Sclerosis? *Bulletin of Mathematical Biology*, **85**, Article No. 75. https://doi.org/10.1007/s11538-023-01181-0

[6] Dendrou, C.A., Fugger, L. and Friese, M.A. (2015) Immunopathology of Multiple Sclerosis. *Nature Reviews Immunology*, **15**, 545-558. https://doi.org/10.1038/nri3871

[7] Polman, C.H., Reingold, S.C., Banwell, B., Clanet, M., Cohen, J.A., Filippi, M., *et al.* (2011) Diagnostic Criteria for Multiple Sclerosis: 2010 Revisions to the McDonald Criteria. *Annals of Neurology*, **69**, 292-302. https://doi.org/10.1002/ana.22366

[8] Alexander, H.K. and Wahl, L.M. (2010) Self-Tolerance and Autoimmunity in a Regulatory T Cell Model. *Bulletin of Mathematical Biology*, **73**, 33-71. https://doi.org/10.1007/s11538-010-9519-2

[9] Zhang, W., Wahl, L.M. and Yu, P. (2014) Modeling and Analysis of Recurrent Autoimmune Disease. *SIAM Journal on Applied Mathematics*, **74**, 1998-2025. https://doi.org/10.1137/140955823

[10] Zhang, W., Wahl, L.M. and Yu, P. (2014) Viral Blips May Not Need a Trigger: How Transient Viremia Can Arise in Deterministic In-Host Models. *SIAM Review*, **56**, 127-155. https://doi.org/10.1137/130937421

[11] Jeschke, J.M., Kopp, M. and Tollrian, R. (2002) Predator Functional Responses: Discriminating between Handling and Digesting Prey. *Ecological Monographs*, **72**, 95-112. https://doi.org/10.1890/0012-9615(2002)072[0095:pfrdbh]2.0.co;2

[12] Dawes, J.H.P. and Souza, M.O. (2013) A Derivation of Holling's Type I, II and III Functional Responses in Predator-Prey Systems. *Journal of Theoretical Biology*, **327**, 11-22. https://doi.org/10.1016/j.jtbi.2013.02.017

[13] Yu, P. (2005) Closed-Form Conditions of Bifurcation Points for General Differential Equations. *International Journal of Bifurcation and Chaos in Applied Sciences and Engineering*, **15**, 1467-1483. https://doi.org/10.1142/s0218127405012582

[14] Hinrichsen, D. and Pritchard, A.J. (2004) Mathematical Systems Theory I: Modelling,

State Space Analysis, Stability and Robustness. Springer.

[15] Xie, J.H., Le, Y. and Li, D. (2018) Nonlinear Dynamics. Science Press.

[16] Lucchinetti, C., Brück, W., Parisi, J., Scheithauer, B., Rodriguez, M. and Lassmann, H. (2000) Heterogeneity of Multiple Sclerosis Lesions: Implications for the Pathogenesis of Demyelination. *Annals of Neurology*, **47**, 707-717. https://doi.org/10.1002/1531-8249(200006)47:6<707::aid-ana3>3.0.co;2-q

[17] Roncador, G., Brown, P.J., Maestre, L., Hue, S., Martínez-Torrecuadrada, J.L., Ling, K., *et al.* (2005) Analysis of FOXP3 Protein Expression in Human CD4+ CD25+ Regulatory T Cells at the Single-Cell Level. *European Journal of Immunology*, **35**, 1681-1691. https://doi.org/10.1002/eji.200526189

[18] Vélez de Mendizábal, N., Carneiro, J., Solé, R.V., Goñi, J., Bragard, J., Martinez-Forero, I., *et al.* (2011) Modeling the Effector-Regulatory T Cell Cross-Regulation Reveals the Intrinsic Character of Relapses in Multiple Sclerosis. *BMC Systems Biology*, **5**, Article No. 114. https://doi.org/10.1186/1752-0509-5-114

[19] Baecher-Allan, C. and Hafler, D.A. (2006) Human Regulatory T Cells and Their Role in Autoimmune Disease. *Immunological Reviews*, **212**, 203-216. https://doi.org/10.1111/j.0105-2896.2006.00417.x

[20] Putnam, A.L., Brusko, T.M., Lee, M.R., Liu, W., Szot, G.L., Ghosh, T., *et al.* (2009) Expansion of Human Regulatory T-Cells from Patients with Type 1 Diabetes. *Diabetes*, **58**, 652-662. https://doi.org/10.2337/db08-1168